NATIONAL ADVISORY COMMITTEE FOR AERONAUTICS

TECHNICAL NOTE 3210

THE ROLE OF TRIPLE COLLISIONS IN EXCITATION OF MOLECULAR VIBRATIONS IN NITROUS OXIDE

By Richard A. Walker, Thomas D. Rossing, and Sam Legvold

Iowa State College

Washington
May 1954

1E

NATIONAL ADVISORY COMMITTEE FOR AERONAUTICS

TECHNICAL NOTE 3210

THE ROLE OF TRIPLE COLLISIONS IN EXCITATION OF MOLECULAR VIBRATIONS IN NITROUS OXIDE

By Richard A. Walker, Thomas D. Rossing, and Sam Legvold

SUMMARY

The basic problem in the research described in this report has been concerned with a determination of the importance of triple collisions in the thermal relaxation process (heat capacity lag) of gaseous mixtures. The experimental program involved the measurement at ultrasonic frequencies of the velocity of sound in mixtures of the basic dispersive gas nitrous oxide N_2O and impurity gases nitrogen N_2, helium He, and argon A. Wide ranges of pressures and concentrations for the gas mixtures were required in the experiments to ascertain the possible effects of triple collisions.

Results of the experiments have shown that the thermal relaxation times of the gas mixtures studied can be very well explained on the basis of binary collisions alone and that triple collisions do not play a discernible part in the excitation of molecular vibrations.

The rudiments of the theory of sound dispersion and relaxation phenomena are presented along with an analysis of the manner in which the effects of triple collisions might be determined.

INTRODUCTION

In the ultrasonic region, the velocity of sound is not constant with respect to frequency. The accepted explanation is that the excitation and deexcitation of molecular vibrations fail to follow very rapid acoustic cycles. Hence at high frequencies the vibrational specific heat of a gas lags, and the lowered heat capacity of the gas gives rise to a higher sonic velocity. For similar reasons, a high anomalous absorption occurs in the same frequency range.

It is a well-known experimental fact that the presence of certain impure molecules, even in very small proportions, greatly reduces the

"relaxation time" of the vibrational energy (i.e., the time necessary for the departure from thermal equilibrium to be reduced to 1/e of its initial value). A satisfactory explanation of this "trace catalyst" phenomenon has not been given. The phenomenon is described more fully in a previous paper (ref. 1).

Very little experimental work has been done using high concentrations of added gases. Walker (ref. 2) has observed that some previous data could be explained nicely by attaching a relatively large importance to the effect of triple collisions.

In the studies reported in this paper, varying concentrations of helium He, argon A, and nitrogen N_2 have been added to nitrous oxide N_2O, and a comparison has been made between the roles played by double and triple collisions in the excitation of vibrational energy.

This work was conducted at Iowa State College under the sponsorship and with the financial assistance of the National Advisory Committee for Aeronautics.

SYMBOLS

a,b	Van der Waals' gas constants
C	molecular steric factor
C_o	molar heat capacity at constant volume below dispersive region
C_p	molar heat capacity at constant pressure below dispersive region
C_∞	molar heat capacity at constant volume above dispersive region
C_{rot}	molar heat capacity at constant volume due to rotational energy of molecules
C_{trans}	molar heat capacity at constant volume due to translational energy of molecules
C_{vib}	molar heat capacity at constant volume due to vibrational energy of molecules
C_ω	molar heat capacity at constant volume at angular frequency ω in dispersive region

f	acoustic frequency
f_{inf}	acoustic frequency at which inflection point of velocity dispersion curve lies
h	Planck's constant
K	coefficient of thermal conductivity
k	Boltzmann's constant
M	molecular weight
m	reduced mass of two colliding molecules
N_o	Avogadro's number
p	pressure
R	universal gas constant
R.P.	real part of a complex number
S	range of intermolecular forces
T	absolute temperature
V	phase velocity of sound
V_c	complex velocity of sound
V_{ideal}	velocity of sound for an ideal gas
V_o	sonic velocity at frequencies below dispersive region
V_{VDW}	velocity of sound for a Van der Waals gas
V_∞	sonic velocity at frequencies above dispersive region
v	molar volume
α	intensity absorption coefficient, per centimeter
α_{cl}	classical absorption coefficient, per centimeter
α_{relax}	absorption coefficient, per centimeter, due to thermal relaxation
γ	ratio of C_p to C_o

η coefficient of viscosity

θ vibrational relaxation time of pure gas

$\overline{\theta}$ vibrational relaxation time of gas mixture

$\theta_{AA}, \theta_{AB}, \ldots$ vibrational relaxation times due to one type of collision only; explained in text of paper

λ acoustic wave length

$\mu = \mu_{cl} + \mu_{relax}$

μ_{cl} intensity absorption coefficient, per wave length, due to viscosity and heat conduction

μ_{max} maximum value of μ_{relax}

μ_{relax} intensity absorption coefficient, per wave length, due to vibrational relaxation

ν frequency of molecular vibration

ξ velocity correction due to absorption

ρ mass density

φ fractional particle concentration of B gas in mixture

ω angular frequency of sound, $2\pi f$

ω_{inf} angular frequency at which inflection point of velocity dispersion curve lies

ω_{max} angular frequency at which μ_{max} occurs

BRIEF THEORY OF SONIC DISPERSION

Richards (ref. 3) derives a useful formula for the velocity of sound. Neglecting the effect of finite amplitudes on velocity (which, at ordinary acoustic levels, produce changes of less than 0.001 percent), he writes:

$$V^2 = \left(\frac{\partial p}{\partial \rho}\right)_T + \left(\frac{\partial p}{\partial T}\right)^2 \frac{MT}{\rho^2 C_o} \qquad (1)$$

For an ideal gas this leads to the familiar expression:

$$V_{ideal}^2 = \frac{RT}{M}\left(1 + \frac{R}{C_o}\right) = \frac{\gamma p}{\rho} \tag{2}$$

However, even at atmospheric pressure, velocities in most gases deviate from the above value by about $\frac{1}{2}$ percent because of nonideal behavior. A well-accepted equation of state is one due to Van der Waals:

$$p = \frac{RT}{v - b} - \frac{a}{v^2} \tag{3}$$

where a and b are usually determined experimentally for each gas. Substitution of this equation into equation (1), neglecting terms in ρ^2, yields:

$$V_{VDW}^2 = \frac{RT + p\left(b - \frac{2a}{RT}\right)}{M - b\rho} + \frac{R}{C_o}\frac{RT}{M - 2b\rho} \tag{4}$$

The above relations assume no absorption of sound in the transmitting medium. When sound is propagated through an absorbing medium, the velocity of propagation is affected. Richards (ref. 3) derives the equation which describes this effect:

$$R.P.\left(V_c^2\right) = \frac{1 - \frac{(2\alpha)^2 V^2}{\omega^2}}{1 + \frac{(2\alpha)^2 V^2}{\omega^2}} V^2 = \xi V^2 \tag{5}$$

in which V denotes the real observed phase velocity and the real part of the quantity V_c^2 gives the square of the velocity calculated for the medium; α is the intensity absorption coefficient per centimeter.

In general, absorption is due to both classical effects and thermal relaxation; that is:

$$\alpha = \alpha_{cl} + \alpha_{relax} \tag{6}$$

where α_{cl} is the classical absorption per centimeter observed by Stokes and Kirchoff:

$$\alpha_{cl} = \frac{2\pi^2 f^2}{\rho V^3}\left(\frac{4}{3}\eta - \frac{\gamma - 1}{C_p}K\right) = \mu_{cl}\lambda \tag{7}$$

where K is the coefficient of thermal conductivity. Richards (ref. 3) develops a formula for absorption per wave length due to relaxation effects:

$$\mu_{relax} = \frac{\alpha_{relax}}{\lambda} = 2\pi\omega\theta\left[\frac{R(C_o - C_\infty)}{C_o(C_o + R) + \omega^2\theta^2 C_\infty(R + C_\infty)}\right] \tag{8}$$

the derivation of which will become clearer in a later section.

Since α is used only to calculate ξ, it is not necessary to recalculate μ_{relax} using a Van der Waals gas. For one of the most absorbing gases known, carbon disulfide, $R.P.\left(V_c^2\right)$ differs from the real phase velocity by about 0.17 percent.

The foregoing theory of "classical" sound propagation in ideal and real gases has assumed a constant velocity at all frequencies (except as α depends upon frequency). That such is not true at all frequencies has already been established qualitatively.

In ordinary gases at temperatures below 2,000° C (so that molecular dissociation and electronic excitation effects are negligible), the specific heat of a gas at constant volume is given by:

$$C_o = C_{trans} + C_{rot} + C_{vib} \tag{9}$$

At high sonic frequencies, as has been pointed out, excitation of vibrational energy does not follow the rapid adiabatic acoustic cycle, and C_{vib} drops out. If the specific heat at frequencies above the dispersive region is denoted by C_∞ and that below this region by C_o, one may write:

$$C_\infty = C_{trans} + C_{rot} \tag{10}$$

$$C_o = C_\infty + C_{vib} \tag{11}$$

For intermediate frequencies, again a formula is borrowed from Richards (ref. 3):

$$C_\omega = C_\infty + \frac{C_o - C_\infty}{1 + i\omega\theta} \tag{12}$$

in which θ is the vibrational relaxation time of the gas (see "Introduction").

If these values are substituted into equations (2) and (5), one obtains for an ideal gas:

$$V_\infty^2 = \frac{RT}{M}\left(1 + \frac{R}{C_\infty}\right) \tag{13}$$

$$V_o^2 = \frac{RT}{M}\left(1 + \frac{R}{C_o}\right) \tag{14}$$

$$\S V_{ideal}^2 = \frac{RT}{M}\left(1 + R\,\frac{C_o + \omega^2\theta^2 C_\infty}{C_o^2 + \omega^2\theta^2 C_\infty^2}\right) \tag{15}$$

Correspondingly, for a Van der Waals gas:

$$\S V_{VDW}^2 = \frac{RT + p\left(b - \frac{2a}{RT}\right)}{M - b\rho} + \frac{R^2T}{M - 2b\rho}\,\frac{C_o + \omega^2\theta^2 C_\infty}{C_o^2 + \omega^2\theta^2 C_\infty^2} \tag{16}$$

Thermal relaxation is usually effective over a range of more than 6 octaves and exists in a different region for each gas or gas mixture, making experimental techniques of measurement quite difficult. The angular frequency at which the inflection point of the velocity curve occurs is given by:

$$\omega_{inf} = C_o/\theta C_\infty \tag{17}$$

and the frequency of maximum absorption by:

$$\omega_{max} = \frac{C_o V_o}{\theta C_\infty V_\infty} \tag{18}$$

Since V_o and V_∞ differ only by a few percent, the two frequencies are quite close for most gases. Typical plots of V^2 and μ as functions of ω are shown in figure 1.

Fortunately, V_o, V_∞, and μ_{max} do not depend upon the relaxation time θ. Changes in gas composition, which are small enough to leave M appreciably unchanged, do not therefore change the shape of the dispersion curve but merely displace the curve along the frequency axis. Thus fewer measurements are necessary to establish the dispersive curve for a given gas or mixture.

A discussion of collision rates and the theoretical basis of relaxation times involves some rather lengthy theory and will be omitted from this report. Walker's doctoral thesis (ref. 4) contains an outline of the work which has been done on this problem. Expressions for the pressure and temperature dependence of relaxation times and therefore the sonic frequency result from such theory.

It is through the dependence of the collision rate on pressure that the pressure dependence of the relaxation time θ is introduced. It can be shown that, if vibrational excitation is solely the result of double collisions, θ should be inversely proportional to the pressure and therefore ω_{max} and ω_{inf}, proportional to pressure. If, on the other hand, triple collisions are primarily responsible, as Walker (ref. 2) has suggested, the dependence of the above quantities should be dependent upon the square of the pressure.

The importance of studies to determine the roles of various types of collision is brought out by the above discussion. Graphs such as figure 1 might easily be drawn with $\log_e \omega/p$ or $\log_e \omega/p^2$ respectively, as abscissa, depending upon whether double or triple collisions are more important. The graph could then be drawn with greater accuracy because the pressure can be varied continuously, whereas the frequency variation is limited by the number of different crystals available. First, however, the relative importance of the two collision types must be determined. In an ideal gas V_o and V_∞ would be independent of pressure; in a real gas they are not quite independent because of interaction forces. Thus V_o and V_∞ have a relatively small dependence on pressure.

The dependence of sonic velocity on temperature is a little more complex since V_∞, V_o, and θ are all functions of T. The dependence of θ on T is given by:

$$\theta = \frac{1}{\frac{N_o S}{R}\frac{p}{T}\left(\frac{8kT}{\pi m}\right)^{1/2} C\sigma(T) e^{-\sigma(T)}\left(1 - e^{-h\nu/kT}\right)} \tag{19}$$

in which σ, also temperature dependent, is given by:

$$\sigma(T) = \frac{3}{2}\left(\frac{S}{b}\right)^{2/3}\left(\frac{h\nu}{kT}\right)^{1/3} \tag{20}$$

S being the range of intermolecular forces and

$$b = \left(\frac{h}{4\pi^2 m\nu}\right)^{1/2} \tag{21}$$

In equation (19), C represents the so-called "steric factor" and m, the reduced mass of two colliding molecules.

The velocity, as shown in equations (15) and (16), depends explicitly on $T^{1/2}$, and, in addition, C_{vib} is an involved function of T. The relative importance of these three effects in determining the temperature dependence of V varies with different gases. Figures 2 and 3 show typical calculated curves for N_2O.

In a mixture made up of φ parts of gas B and $1 - \varphi$ parts of gas A, it can be shown that

$$\frac{1}{\bar{\theta}} = \frac{1 - \varphi}{\theta_{AA}} + \frac{(1 - \varphi)^2}{\theta_{AAA}} + \frac{\varphi}{\theta_{AB}} + \frac{\varphi(1 - \varphi)}{\theta_{AAB}} + \frac{\varphi^2}{\theta_{ABB}} \tag{22}$$

represents the observed relaxation time in terms of the relaxation times due to various types of collisions. In the above equation:

$\bar{\theta}$ relaxation time observed

θ_{AA} relaxation time due to collisions between two A molecules

θ_{AAA} relaxation time due to collisions between three A molecules

θ_{AB} relaxation time due to collisions between one A and one B molecule

θ_{AAB} relaxation time due to collisions between two A and one B molecule

θ_{ABB} relaxation time due to collisions between one A and two B molecules

Most investigators have assumed that triple collisions are not relatively important and write equation (22) thus:

$$\frac{1}{\bar{\theta}} = \frac{1 - \varphi}{\theta_{AA}} + \frac{\varphi}{\theta_{AB}} \tag{23}$$

Eucken and Aybar (ref. 5) modified the equation to fit their data in mixtures of carbonyl sulfide and nitrogen and of carbonyl sulfide and argon:

$$\frac{1}{\bar{\theta}} = \frac{(1 - \varphi)^2}{\theta_{AA}} + \frac{\varphi(1 - \varphi)}{\theta_{AB}} \tag{24}$$

and give a theoretical argument in favor of their equation. Walker (ref. 2) pointed out that their data would also fit an equation derived from equation (22) by neglecting the effects of AAA, AB, and ABB collisions:

$$\frac{1}{\bar{\theta}} = \frac{1 - \varphi}{\theta_{AA}} + \frac{\varphi(1 - \varphi)}{\theta_{AAB}} \tag{25}$$

Previous to the Iowa State investigation, the limited data of Eucken and Aybar were the only data on mixtures with relatively large B gas concentrations, and definite conclusions could not be drawn.

DESCRIPTION OF APPARATUS

The interferometer used is patterned after one described by Telfair and Pielemeier (ref. 6) with a number of modifications. The interferometer is designed to work at pressures from 0 to 3 atmospheres and from room temperature to 450° C. The chamber and most of the gas-handling equipment are constructed of corrosion-resistant stainless steel.

Seven X-cut quartz crystals cover a frequency range of 200 to 1,500 kilocycles in steps of approximately 1/2 octave. All the crystals used have been 5 centimeters in diameter, since it has been found that annoying diffraction effects can be noticed if the transducer diameter is of the order of the wave length (which is usually less than 1 millimeter). Crystal noise was found to be minimized by clamping the crystals with three screws in their nodal planes. Contact was made with the crystal by painting a conductive coating from two of these screws to opposite faces of the crystal.

The interferometer and associated equipment are shown in figure 4. On the left are gas cylinders and pressure gages. On the table top are a desiccating chamber and systems of Kerotest diaphragm valves to control the flow of gases. A vacuum pump, capable of evacuating the entire system to 0.1 micron, is mounted under the table top. The interferometer is at the right of the table. A removable oven has been lowered, in the figure, to show the test chamber.

The studies in this paper were performed slightly above room temperature and the oven was replaced by a thermostatically controlled water bath heated by an infrared lamp.

The gas-handling system is shown in figure 5. Gases whose moisture content is objectionable can be stored under pressure in contact with phosphorus pentoxide P_2O_5 in the drying chamber. A liquid-nitrogen cold trap is used to remove noncondensable gases such as nitrogen and argon.

Figure 6 shows the details of the chamber. The acoustic reflector is an optically flat stainless steel disk mounted on the end of an Invar rod. To maintain parallelism between the reflector and crystal surface, the Invar rod has been precision ground and moves through a bearing with 0.0001-inch clearance. A Gaertner micrometer slide with a least count of 0.001 millimeter is used to drive the rod and reflector in a vertical direction and can be seen at the top of the interferometer. A special adjustable mounting plus a counterweight minimize strains in the micrometer and rod.

To achieve the desired precision, it is necessary to set the reflector and crystal face very nearly parallel. This can be done by adjusting three micrometer screws on the crystal mounting table. Optically flat crystals have been tried; but, because of difficulties encountered due to the poor adherence of crystal plating on such polished surfaces, etched crystals have replaced them at all but the highest frequencies.

The crystal oscillator used is a variation of a circuit due to Boella (ref. 7), and it is described by Rossing (ref. 8). Precision parts are used throughout, and, to reduce noise levels further, battery power is used. In order to detect changes in the acoustic field as the reflector is displaced, a sensitive microammeter is placed in the plate supply of the oscillator stage and bypassed with a constant current. Thus it is possible to detect changes in the plate current of 1 part in 10,000, thermal noise being about this magnitude.

Frequency is measured by beating the output of the crystal (or one of its harmonics) against the carrier of a commercial broadcast station. By comparing the beat note produced with the output of an audio oscillator, an accuracy of 1 part in 20,000 is achieved.

Pressures from 0.5 millimeter of mercury to 3 atmospheres can be measured with a two-meter U-tube manometer. Pressures of 0.1 micron to 250 microns (0.0001 to 0.25 millimeter) of mercury are read on a McLeod vacuum gage.

Temperature measurements have been made with a good quality mercury thermometer. Provisions have been made to use a platinum resistance thermometer in the chamber, but this has not yet been found necessary. Temperature control at elevated temperatures is effected by a Brown-Honeywell automatic regulator. For room temperature measurements a mercury thermostat, used with an infrared heating bulb and a Cenco stirrer, keeps the water-bath temperature constant to within $\pm 0.1^{\circ}$ C.

The gases used in the experiment, except helium, were supplied by Matheson Co., Inc., and were of the highest purity available. The helium used was Bureau of Mines Grade A gas. The nitrous oxide used was purified by freezing with liquid oxygen and pumping off nitrogen, the principal impurity.

EXPERIMENTAL PROCEDURE AND RESULTS

Percentage concentrations were determined by reading the partial pressure of each gas and the total pressure of the mixture. The assumption was made that the partial pressures were additive (which is a good approximation even for a Van der Waals gas). Gases were allowed to mix for about 24 hours before measurements were taken.

When measurements were made near the frequency of maximum absorption, only 25 to 30 nodes could be measured. In other cases as many as 70 were measurable. Since errors in frequency measurement are very small, velocity measurements were as correct as the wave lengths measured, or to about 1 part in 10,000.

During the calibration of the interferometer with research-grade argon, a nondispersive gas of unusually high purity, an anomaly was apparent in the acoustic field. Measured velocities were found to differ from the theoretical ones by 9 to 17 parts in 10,000, depending upon the position in the cup at which measurements were made. This anomaly was later found to be due largely to errors in temperature measurement, although certain authors have pointed out that standing waves may not be exactly half wave lengths apart. Appropriate corrections were applied to the measured velocities to compensate for these errors.

The second correction applied to the data was that due to absorption which has been already discussed. Values of μ were calculated from equation (8) and used to calculate ξ, the correction factor for absorption.

Measurements of the velocity were made with B molecule concentrations of 10, 20, 30, and 50 percent added to nitrous oxide, the basic gas. The raw data are shown in table I. Since V_0 and V_∞, the velocities at very low and very high frequencies, are independent of the relaxation time, it is convenient to draw a velocity dispersion curve from equation (16) using an approximate value of θ, the relaxation time, and merely displace it along the axis of abscissas to give the best fit with the experimental data.

These curves, so drawn, will be different for each concentration because of the dependence of the velocity on the molecular weight and Van der Waals' constants a and b of the gas mixture. The latter can be determined fairly accurately from relations given by Glasstone (ref. 9, p. 298):

$$\left.\begin{aligned} \sqrt{a_m} &= (1 - \varphi)\sqrt{a_A} + \varphi\sqrt{a_B} \\ b_m &= (1 - \varphi)\, b_A + \varphi b_B \end{aligned}\right\} \tag{26}$$

where the subscripts m, A, and B refer to the mixture and the A and B components, respectively. In plotting these curves ξ, the correction for absorption, was set equal to unity. For the curves cited, an approximate relaxation time of 10^{-6} second was used.

The velocity measurements at each frequency were corrected for the effect of absorption and for the errors indicated by the argon calibration. After the theoretical dispersion curve was displaced along the frequency axis to give the best fit with these corrected velocities, the frequency at which the inflection point lay was determined from the graph. Application of equation (17) then gave θ, the relaxation time.

Figure 7 shows a typical graphical determination of θ. The corrected velocities, measured at frequencies of 300, 600, and 1,000 kilocycles per second, are plotted as open circles and the real-gas curve has been positioned to give the best fit with these measurements. An ideal-gas dispersion curve for this mixture has been drawn and its inflection point indicated. Since the real-gas curve is slightly asymmetrical, no inflection point can be determined. The inflection point of the corresponding ideal-gas curve is, however, indicated by a cross just to the left of the real-gas curve.

Values of f_{inf}, graphically determined, are given in table II together with the values of $\overline{\theta}$ calculated from them. In light of small errors indicated by the argon calibration, the values of $\overline{\theta}$ are probably correct to about 3 to 5 percent.

Table III shows the values of θ_{AB} calculated from $\overline{\theta}$ using equations (23) and (24) (proposed by Eucken and Aybar) and also values of θ_{AAB} calculated from equation (25). If double collisions only are important, θ_{AB} should be independent of percentage concentrations. If excitation is due to triple collisions only, θ_{AAB} should be constant for given constituents. Also in pure N_2O, if double collisions are solely responsible, relaxation time should double as pressure is halved. This is exactly what happens. From table III it is concluded that AB collisions are principally responsible for vibrational excitation in N_2O-N_2 and in N_2O-He mixtures. In N_2O-A mixtures it is very difficult to evaluate the respective roles of AB and AAB collisions.

The vibrational relaxation time measured in pure N_2O, $\theta = 0.93 \times 10^{-6}$ second, agrees very well with that reported by Eucken and Jaacks (ref. 10), who measured 0.92×10^{-6} second. On the other hand, Fricke (ref. 11) reports a value of 1.44×10^{-6} second. Fricke's measurements, however, were made at a frequency well below the frequencies of the present investigations.

Iowa State College,
Ames, Iowa, May 26, 1953.

REFERENCES

1. Walker, Richard: Heat Capacity Lag in Gases. NACA TN 2537, 1951.

2. Walker, Richard A.: On the Interpretation of Relaxation Time Measurements in Gas Mixtures. Jour. Chem. Phys., vol. 19, no. 4, Apr. 1951, pp. 494-497.

3. Richards, William T.: Supersonic Phenomena. Rev. Modern Phys., vol. 11, no. 1, Jan. 1939, pp. 36-64.

4. Walker, Richard Alden: Role of Triple Collisions in Excitation of Molecular Vibrations. Ph. D. Thesis, Iowa State College, 1952.

5. Eucken, A., and Aybar, S.: Die Stossanregung intramolekularer Schwingungen in Gasen und Gasmischungen. VI - Schallabsorptions- und dispersions Messungen an CH_4, COS und ihren Mischungen mit Zusatzgasen. Zs. phys. Chemie, Abl. B, Bd. 46, Nr. 4, June 1940, pp. 195-211.

6. Telfair, D., and Pielemeier, W. H.: An Improved Apparatus for Supersonic Velocity and Absorption Measurements. Rev. Sci. Instr., vol. 13, no. 3, Mar. 1942, pp. 122-126.

7. Boella, M.: Performance of Piezo-Oscillations and the Influence of the Decrement of Quartz on the Frequency of Oscillations. Proc. Inst. Radio Engs., vol. 19, no. 7, July 1931, pp. 1252-1277.

8. Rossing, T. D.: An Oscillator for Acoustic Interferometry. M. S. Thesis, Iowa State College, 1952.

9. Glasstone, Samuel: Textbook of Physical Chemistry. D. Van Nostrand Co., Inc., 1940.

10. Eucken, A., and Jaacks, H.: Die Stossanregung intramolekularer Schwingungen in Gasen und Gasmischungen auf Grund von Schalldispersionmessungen. III - Messungen an Stickoxydul. Zs. phys. Chemie, Abl. B, Bd. 30, Nr. 2/3, Oct. 1935, pp. 85-112.

11. Fricke, E. F.: The Absorption of Sound in Five Triatomic Gases. Jour. Acous. Soc. Am., vol. XII, no. 2, Oct. 1940, pp. 245-254.

TABLE I

MEASURED AND CORRECTED SONIC VELOCITIES

Gas	Measured velocity, V, m/sec	V^2, $(m/sec)^2$	V^2 corrected in terms of argon calibration, $(m/sec)^2$
Frequency, 500 kcps			
2 atm N_2O	270.90	7.528×10^4	7.515×10^4
1 atm N_2O	276.11	7.612	7.598
1/2 atm N_2O	279.80	7.823	7.809
1/4 atm N_2O	281.22	7.906	7.892
90.0% N_2O and 10.0% A	279.91	7.824	[a]7.810
80.0% N_2O and 20.0% A	283.90	8.050	[a]8.033
70.0% N_2O and 30.0% A	288.08	8.291	[a]8.273
50.0% N_2O and 50.0% A	297.01	8.817	[a]8.796
90.0% N_2O and 10.0% N_2	282.09	7.947	7.933
80.0% N_2O and 20.0% N_2	288.40	8.309	8.295
70.0% N_2O and 30.0% N_2	295.02	8.697	8.682
50.0% N_2O and 50.0% N_2	309.20	9.557	9.539
90.0% N_2O and 10.0% He	287.73	8.268	8.254
80.0% N_2O and 20.0% He	303.72	9.216	9.199
70.0% N_2O and 30.0% He	324.34	10.514	10.496
50.0% N_2O and 50.0% He	381.37	14.528	14.502
Frequency, 600 kcps			
2 atm N_2O	275.61	7.585×10^4	7.569×10^4
1 atm N_2O	279.52	7.807	7.787
1/2 atm N_2O	281.13	7.901	7.884
1/4 atm N_2O	281.69	7.934	7.917
90.0% N_2O and 10.0% A	282.83	7.996	[a]7.979
80.0% N_2O and 20.0% A	286.43	8.200	[a]8.180
70.0% N_2O and 30.0% A	290.13	8.416	[a]8.395
50.0% N_2O and 50.0% A	298.18	8.889	[a]8.862
90.0% N_2O and 10.0% N_2	283.12	8.125	8.105
80.0% N_2O and 20.0% N_2	290.96	8.462	8.443
70.0% N_2O and 30.0% N_2	297.21	8.831	8.811
50.0% N_2O and 50.0% N_2	310.72	9.653	9.631
90.0% N_2O and 10.0% He	292.27	8.589	8.514
80.0% N_2O and 20.0% He	307.94	9.468	9.451
70.0% N_2O and 30.0% He	327.86	10.755	10.716
50.0% N_2O and 50.0% He	385.77	14.717	14.691
Frequency, 1,000 kcps			
2 atm N_2O	278.11	7.728×10^4	7.704×10^4
1 atm N_2O	280.63	7.874	7.851
1/2 atm N_2O	281.45	7.920	7.899
1/4 atm N_2O	281.75	7.938	7.920
90.0% N_2O and 10.0% A	283.63	8.043	[a]8.022
80.0% N_2O and 20.0% A	287.05	8.238	[a]8.215
70.0% N_2O and 30.0% A	290.68	8.448	[a]8.426
50.0% N_2O and 50.0% A	298.50	8.909	[a]8.881
90.0% N_2O and 10.0% N_2	285.93	8.174	8.153
80.0% N_2O and 20.0% N_2	291.72	8.508	8.486
70.0% N_2O and 30.0% N_2	297.97	8.877	8.854
50.0% N_2O and 50.0% N_2	311.29	9.689	9.664
90.0% N_2O and 10.0% He	294.56	8.669	8.653
80.0% N_2O and 20.0% He	311.12	9.667	9.650
70.0% N_2O and 30.0% He	331.05	10.944	10.926
50.0% N_2O and 50.0% He	386.55	14.938	14.911

[a]For all argon mixtures V^2 also corrected for change in molecular weight of argon caused by nitrogen impurity. Effective M for argon, 39.896.

TABLE II

FREQUENCIES AT WHICH INFLECTION POINTS OF DISPERSION CURVES LIE AND THERMAL RELAXATION TIMES CALCULATED THEREFROM

Gas	f_{inf}, kcps	$\bar{\theta}$, sec
2 atm N_2O	500	0.465×10^{-6}
1 atm N_2O	250	.93 ($=\theta_{AA}$)
1/2 atm N_2O	124	1.87
1/4 atm N_2O	62	3.75
90.0% N_2O and 10.0% A	223	1.02
80.0% N_2O and 20.0% A	194	1.15
70.0% N_2O and 30.0% A	169	1.29
50.0% N_2O and 50.0% A	124	1.65
90.0% N_2O and 10.0% N_2	233	.96
80.0% N_2O and 20.0% N_2	217	1.00
70.0% N_2O and 30.0% N_2	199	1.06
50.0% N_2O and 50.0% N_2	173	1.13
90.0% N_2O and 10.0% He	445	.51
80.0% N_2O and 20.0% He	650	.342
70.0% N_2O and 30.0% He	800	.272
50.0% N_2O and 50.0% He	1,140	.180

TABLE III

COMPARISON OF θ_{AB} AND θ_{AAB} VALUES

Gas mixture	θ_{AB} using eq. (23), sec	θ_{AB} using eq. (24), sec	θ_{AAB} using eq. (25), sec
90.0% N_2O and 10.0% A	1×10^{-6}	0.8×10^{-6}	1×10^{-6}
80.0% N_2O and 20.0% A	2	.9	2
70.0% N_2O and 30.0% A	1	.9	.8
50.0% N_2O and 50.0% A	.7	.7	.35
90.0% N_2O and 10.0% N_2	1.4	.5	1.3
80.0% N_2O and 20.0% N_2	1.4	.5	1.1
70.0% N_2O and 30.0% N_2	1.67	.51	1.11
50.0% N_2O and 50.0% N_2	1.45	.41	.73
90.0% N_2O and 10.0% He	.101	.083	.091
80.0% N_2O and 20.0% He	.097	.072	.078
70.0% N_2O and 30.0% He	.102	.067	.072
50.0% N_2O and 50.0% He	.099	.047	.050

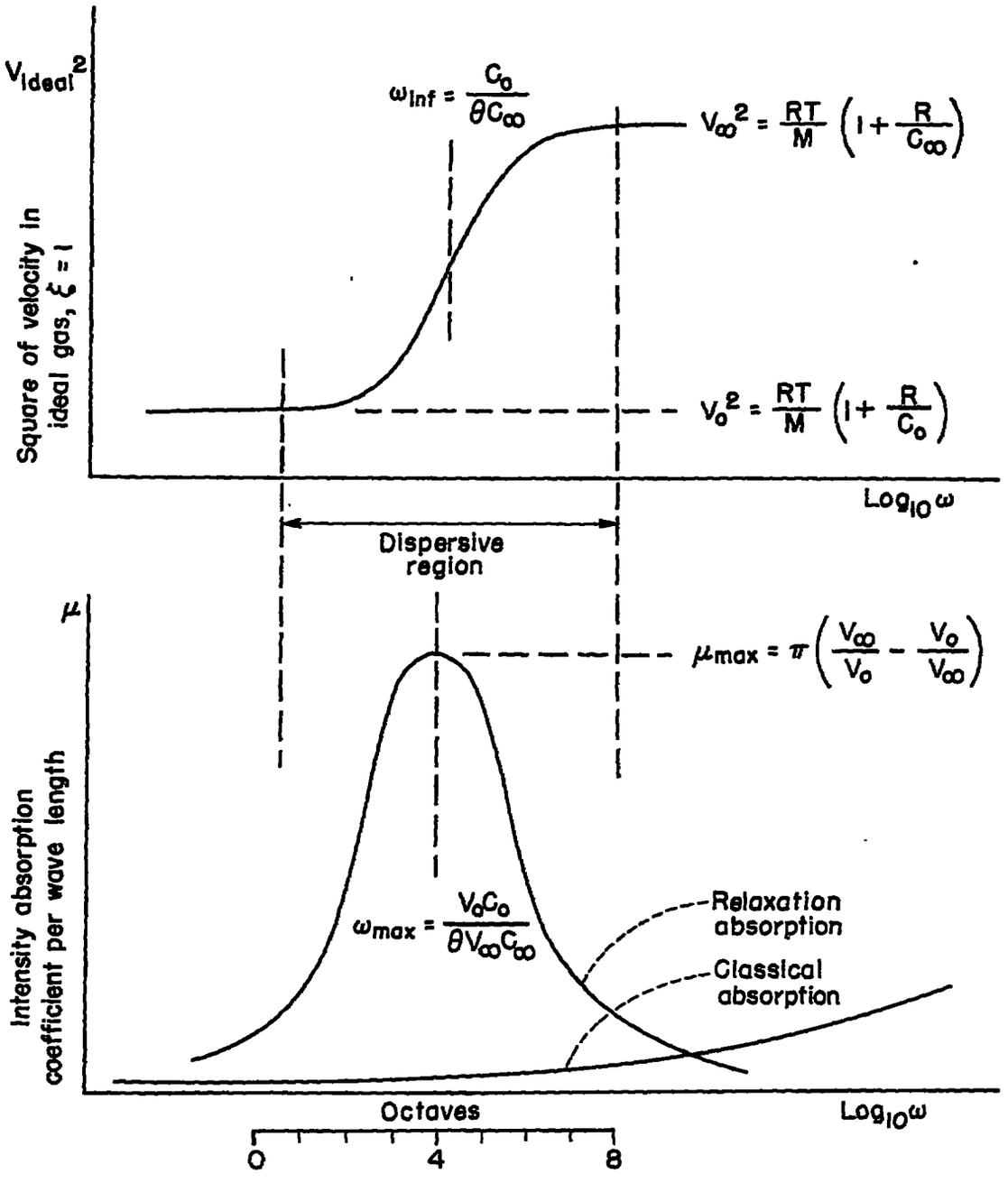

Figure 1.- Sonic velocity and absorption versus frequency for thermal relaxation process.

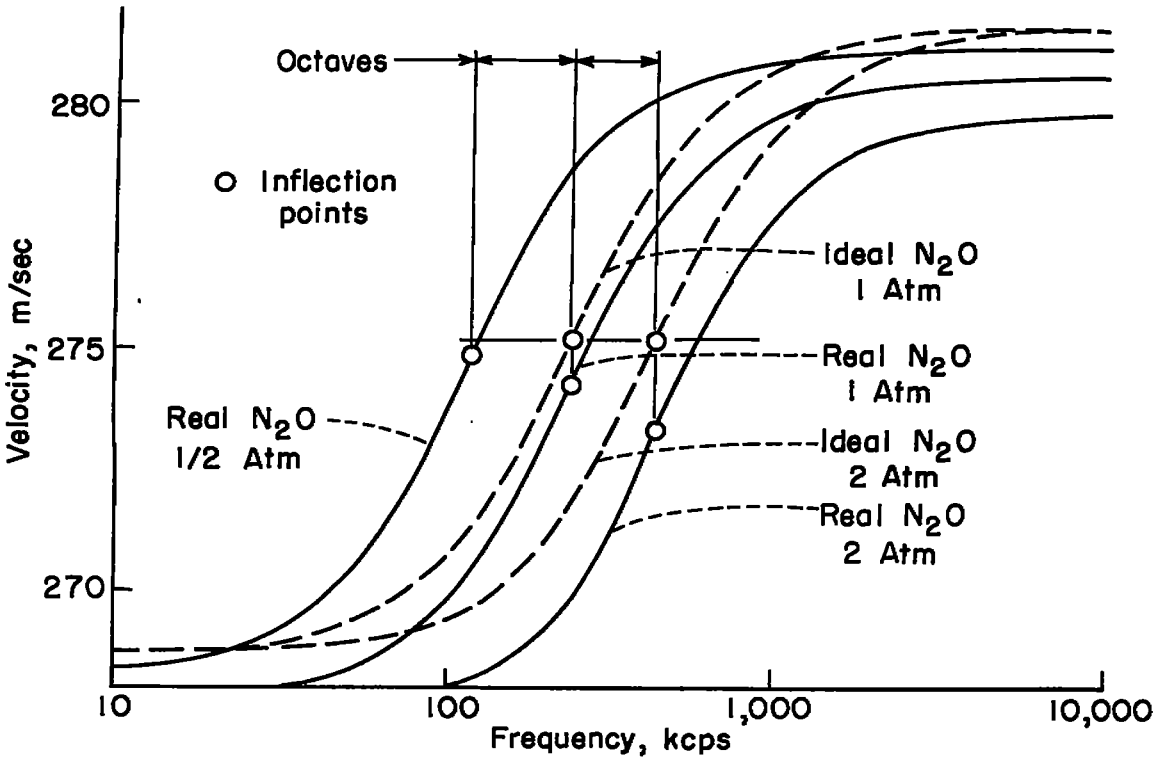

Figure 2.- Sonic velocity in N_2O gas at 27° C.

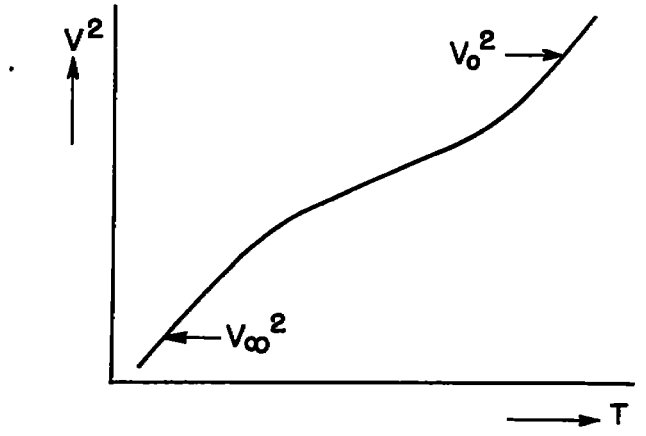

Figure 3.- Isobaric temperature variation of sonic velocity in dispersive gas at constant acoustic frequency.

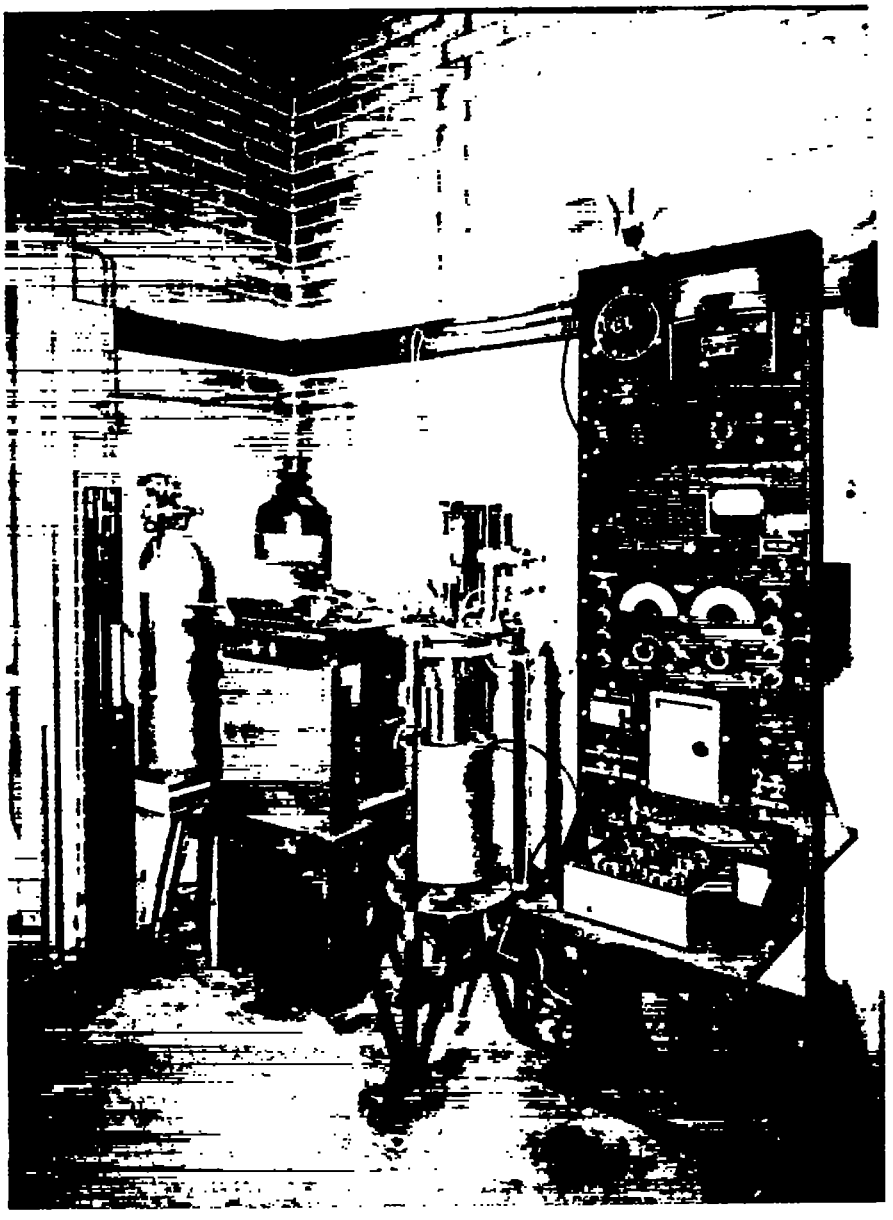

L-82100

Figure 4.- Iowa State ultrasonic interferometer and associated equipment.

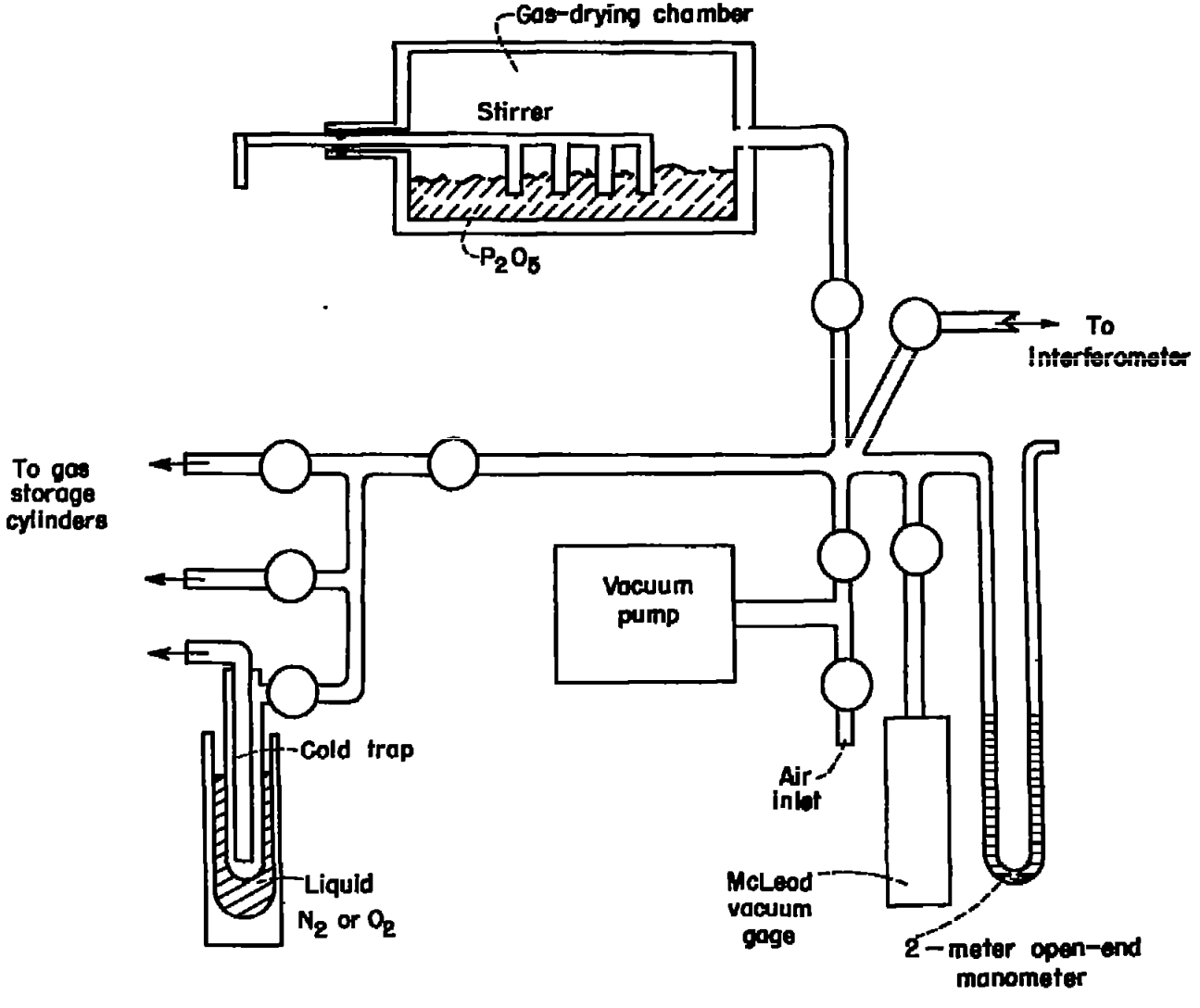

Figure 5.- Gas-handling and vacuum equipment.

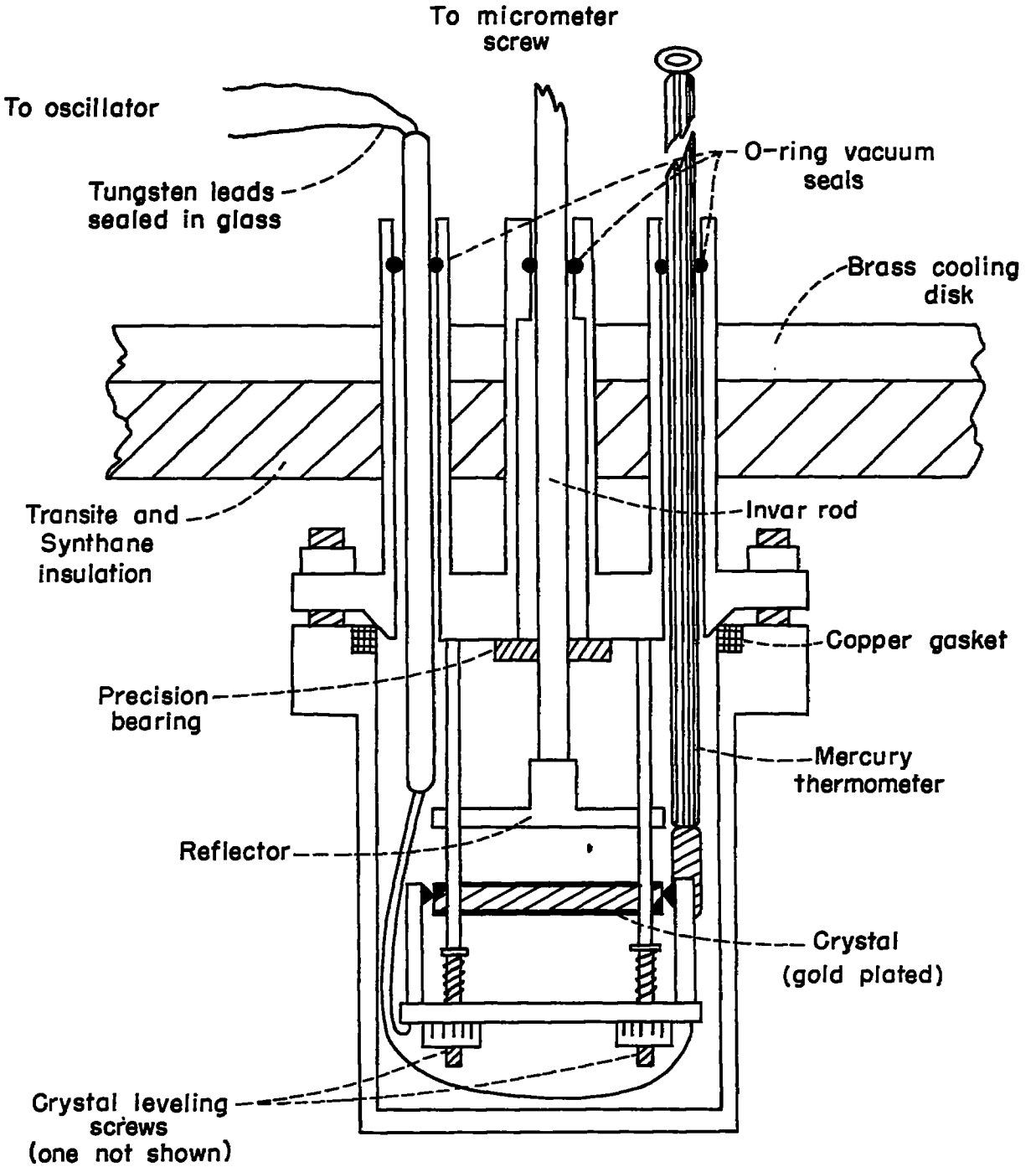

Figure 6.- Interferometer cup showing crystal mounting.

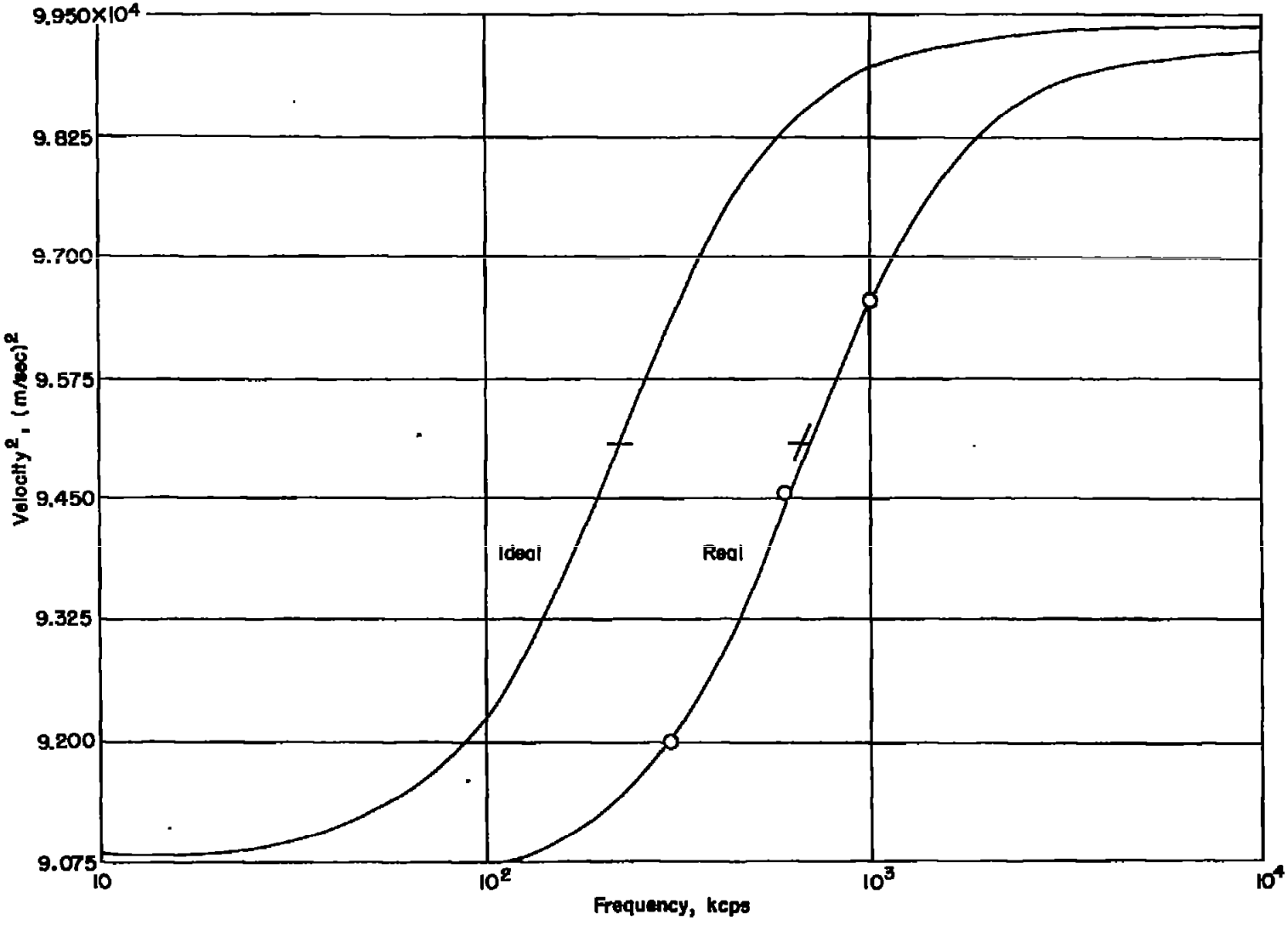

Figure 7.- Velocity measurements in 80 percent N_2O and 20 percent He at 27.0° C.